SUPPLEMENTARY INFORMATION

A. Mesoscopic model of membrane and peripheral proteins

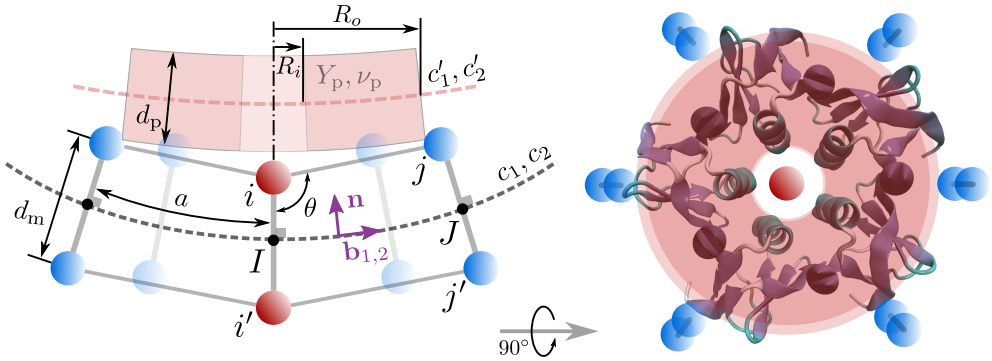

Figure 1: Schematic of the membrane model where a peripheral protein is binding. The discrete geometry of the particle-based model reflects the curvature induced in the membrane. The governing force field is parameterized to reproduce the combined elasticity of the membrane and the protein.

The membrane model used for the simulations presented here, is the same as developed in [1] and used in [2, 3]. The bilayer is modeled as formed by particle-dimers in a close-packed arrangement, with a lattice parameter of a few nanometers, while the two leaflets are resolved (Fig. 1)). Bonded interactions in the model are described via the following potentials [1],

$$U_\mathrm{s}\left(r_{ij}\right) = D_e\left[1 - \exp\left(-\alpha\left(r_{ij} - r_\mathrm{eq}\right)\right)\right]^2 \tag{1a}$$

$$U_\mathrm{a}\left(\theta_{i'ij}\right) = K_a\left(\theta_{i'ij} - \theta_\mathrm{eq}\right)^2 \tag{1b}$$

$$U_\mathrm{d}\left(d_{ii'}\right) = K_d\left(d_{ii'} - d_\mathrm{eq}\right)^2 \tag{1c}$$

Particles belonging to each leaflet are connected to their nearest-neighbour counterparts via Morse-type bonds (Eq. (1a)). Also, harmonic angle-bending potentials given by Eq. (1b) act against the out-of-plane rotations of these bonds. Finally, particles in a dimer are connected via harmonic bonds of the form described by Eq. (1c), which keeps the two leaflets together (Fig. 1)).

As described in the Methods section “Simulations”, the force field masking in the presence of the protein is done such that the underlying membrane model be least affected.

For potentials in Eqs. (1), we modify r_{eq} and θ_{eq} for bonds in top and bottom leaflets. D_{e} and α are left unchanged, leading to α^2/D_{e}, the stiffness of the Morse bond at r_{eq}, to remain constant. The rest of the effects are implemented via the auxiliary angle-bending potential:

$$U'_{\mathrm{a}}\left(\theta_{i'ij}\right) = K'_a\left(\theta_{i'ij} - \theta_{\mathrm{eq}}\right)^2 \tag{2}$$

which reinforces the angle-bending potentials on the top leaflet for the masked particles.

B. Differential geometry of the particle-based model

Consider a locally tangent orthonormal basis constructed at point I on the mid-surface of the membrane (Fig. 1)). Position vectors in this basis are given as $\mathbf{r} = x\,\mathbf{b}_1^I + y\,\mathbf{b}_2^I + z\,\mathbf{n}^I$, in which, $\mathbf{n}^I = \mathbf{b}_1^I \times \mathbf{b}_2^I$ is the surface normal at I. The mid-surface of the membrane can be approximated to the second order through an osculating paraboloid. Assuming the two principal curvatures of the mid-surface to be c_1 and c_2, and the base vector $\mathbf{b}_1^I$ making an angle ϕ with the principal direction corresponding to c_1, the osculating paraboloid is defined via the following relation,

$$\begin{aligned} 2z &= Ax^2 + 2Bxy + Cy^2 \\ A &= H + \frac{c_1 - c_2}{2}\cos 2\phi \\ B &= \frac{c_1 - c_2}{2}\sin 2\phi \\ C &= H - \frac{c_1 - c_2}{2}\cos 2\phi \end{aligned} \tag{3}$$

It can be readily verified that the mean and Gaussian curvatures are given as $H = \frac{1}{2}\left(A + C\right)$ and $G = AC - B^2$. We assume the projection of the bond between particles i and j to be parallel to $\mathbf{b}_1$ (which can always be achieved by a change in the angle ϕ). To find the point J, the projection of the position of particle j on the mid-surface, we assume the mid-surface to be incompressible. Thus, along the $y = 0$ section of the osculating paraboloid, we can find the projection of point j, given by the coordinates $(x_J, 0, z_J)$, assuming it was a distance a apart from I in the undeformed configuration,

$$a = \int_0^{x_J} \sqrt{1 + \left(\frac{\partial z}{\partial x}\right)^2_{y=0}}\, dx = x_J + \frac{A^2}{6}x_J^3 + \mathcal{O}\left(x_J^5\right) \tag{4}$$

discarding x_J^5 and higher-order terms, a closed-form solution is possible. Based on the positions of points I and J, positions of particles i and j are given as,

$$\begin{aligned}\mathbf{r}_i &= \mathbf{r}_I + \frac{d_\mathrm{m}}{2}\mathbf{n}^I \\ \mathbf{r}_j &= \mathbf{r}_J + \frac{d_\mathrm{m}}{2}\mathbf{n}^J \\ &= \mathbf{r}_I + x_J\mathbf{b}_1^I + \frac{Ax_J^2}{2}\mathbf{n}^I + \frac{d_\mathrm{m}}{2}\mathbf{n}^J\end{aligned} \tag{5}$$

where d is the thickness of the membrane and

$$\mathbf{n}_J = \frac{\left(-Ax_J\,\mathbf{b}_1^I - Bx_J\,\mathbf{b}_2^I + \mathbf{n}^I\right)}{\sqrt{1 + A^2x_J^2 + B^2x_J^2}} \tag{6}$$

Having the position of the particle j in the neighborhood of particle i, we can relate the bond-stretching potential between the two (Eq. (1a)) to the curvature of the mid-surface. Similarly, for the out-of-plane angle-bending potential (Eq. (1b)) the triplet of particles $i'\,i\,j$ is considered, with $\mathbf{r}_{i'} = \mathbf{r}_I - \frac{d_\mathrm{m}}{2}\mathbf{n}_I$ (Fig. 1).

C. Force field parametrization

The force field attributed to bonded interactions results in an effective energy density, f_eff. We have estimated this energy density as the ratio of all the potential energies attributed to one particle to the area per particle in the model. We have also averaged this ratio over ϕ to eliminate the effect due to the angle between bonds and the principal directions of the membrane [1]. The force field parameters are obtained via minimizing the loss function,

$$\mathcal{L} = \mathop{\mathbb{E}}_{c_1,c_2}\left[\left(f_\mathrm{eff} - f_\mathrm{tot}\right)^2\right] + \sum_i \lambda_i \mathop{\mathbb{E}}_{c_1,c_2}\left[\left(X_{\mathrm{eff},i} - X_0\right)^2\right] \tag{7}$$

where $X_{\mathrm{eff},i}$'s are other properties for which an effective value can be obtained in the space of inspected membrane geometries.

We chose the Broyden-Fletcher-Goldfarb-Shanno algorithm (BFGS) for parameter-space optimization [4], with the version implemented as part of the Python library SciPy used for this purpose [5]. The physical properties of the membrane and flexible proteins used as input for the optimization are listed in Tab. I. The values of the potential parameters, obtained or chosen for simulations, are summarized in Tab. II.

Table I: Properties of the membrane and peripheral proteins used for the force field parametrization [6–13].

Membrane					
d_m [nm]		κ $[kT]$		$\bar{\kappa}$ $[kT]$	K_area $\left[\mathrm{N\,m^{-1}}\right]$
4.0		18.73		-14.98	0.270
Peripheral protein					
d_p [nm]	R_i [nm]	R_o [nm]	c_0 $\left[\mathrm{nm^{-1}}\right]$	Y_p [MPa]	ν_p
2.92	0.49	3.21	0.08	50, 100, 200	0.25

Table II: Force field parameters for the interaction potentials given in Eqs. (1) and (2).

Unmasked (membrane)		
r_{eq} [nm]	D_{e} $\left[\mathrm{kJ\,mol^{-1}}\right]$	α $\left[\mathrm{nm^{-1}}\right]$
6.5	9.03	0.18
θ_{eq} [rad]	K_{a} $\left[\mathrm{kJ\,mol^{-1}}\right]$	
$\pi/2$	19.35	
d_{eq} [nm]	K_{d} $\left[\mathrm{kJ\,mol^{-1}nm^{-2}}\right]$	
4.0	6.19	

Masked (membrane + protein)			
	$Y_{\mathrm{p}} = 50\,\mathrm{MPa}$		
	r'_{eq} [nm]	θ'_{eq} [rad]	K'_{a} $\left[\mathrm{kJ\,mol^{-1}}\right]$
top leaflet:	5.96	1.70	85.38
bottom leaflet:	7.00	1.44	-
	$Y_{\mathrm{p}} = 100\,\mathrm{MPa}$		
	r'_{eq} [nm]	θ'_{eq} [rad]	K'_{a} $\left[\mathrm{kJ\,mol^{-1}}\right]$
top leaflet:	5.88	1.72	160.37
bottom leaflet:	7.07	1.42	-
	$Y_{\mathrm{p}} = 200\,\mathrm{MPa}$		
	r'_{eq} [nm]	θ'_{eq} [rad]	K'_{a} $\left[\mathrm{kJ\,mol^{-1}}\right]$
top leaflet:	5.67	1.78	232.20
bottom leaflet:	7.24	1.37	-

[1] Sadeghi, M., Weikl, T. R. & Noé, F. Particle-based membrane model for mesoscopic simulation of cellular dynamics. *J. Chem. Phys.* **148**, 044901 (2018).

[2] Sadeghi, M. & Noé, F. Large-scale simulation of biomembranes incorporating realistic kinetics into coarse-grained models. *Nat. Commun.* **11**, 2951 (2020).

[3] Sadeghi, M. & Noé, F. Hydrodynamic coupling for particle-based solvent-free membrane models. *arXiv* 1909.02722 (2020).

[4] Liu, D. C. & Nocedal, J. On the limited memory BFGS method for large scale optimization. *Math. Program.* **45**, 503–528 (1989).

[5] Virtanen, P. *et al.* SciPy 1.0: fundamental algorithms for scientific computing in Python. *Nat. Methods* **17**, 261–272 (2020).

[6] Marsh, D. Elastic curvature constants of lipid monolayers and bilayers. *Chem. Phys. Lipids* **144**, 146–159 (2006).

[7] Hu, M., Briguglio, J. J. & Deserno, M. Determining the Gaussian curvature modulus of lipid membranes in simulations. *Biophys. J.* **102**, 1403–1410 (2012).

[8] Nagle, J. F. Introductory Lecture: Basic quantities in model biomembranes. *Faraday Discuss.* **161**, 11–29 (2013).

[9] Dimova, R. Recent developments in the field of bending rigidity measurements on membranes. *Adv. Colloid Interface Sci.* **208**, 225–234 (2014).

[10] Janosi, L. & Gorfe, A. A. Simulating POPC and POPC/POPG bilayers: Conserved packing and altered surface reactivity. *J. Chem. Theory Comput.* **6**, 3267–3273 (2010).

[11] Klauda, J. B. *et al.* Update of the CHARMM All-Atom Additive Force Field for Lipids: Validation on Six Lipid Types. *J. Phys. Chem. B* **114**, 7830–7843 (2010).

[12] Raghunathan, M. *et al.* Structure and elasticity of lipid membranes with genistein and daidzein bioflavinoids using X-ray scattering and MD simulations. *J. Phys. Chem. B* **116**, 3918–3927 (2012).

[13] Braun, A. R., Sachs, J. N. & Nagle, J. F. Comparing simulations of lipid bilayers to scattering data: The GROMOS 43A1-S3 force field. *J. Phys. Chem. B* **117**, 5065–5072 (2013).